Journal of Geodynamics 105 (2017) 51–61

Contents lists available at ScienceDirect

Journal of Geodynamics

journal homepage: http://www.elsevier.com/locate/jog

Progressive migration of slab break-off along the southern Tyrrhenian plate boundary: Constraints for the present day kinematics

Claudio Chiarabba[a], Mimmo Palano[b,*]

[a] Istituto Nazionale di Geofisica e Vulcanologia, Via di Vigna Murata 605, I-00143 Rome, Italy
[b] Istituto Nazionale di Geofisica e Vulcanologia, Osservatorio Etneo – Sezione di Catania, Piazza Roma 2, I-95125 Catania, Italy

ARTICLE INFO

Article history:
Received 7 March 2016
Received in revised form 20 January 2017
Accepted 22 January 2017
Available online 25 January 2017

Keywords:
Mantle tomography
Strain-rates
Slab break-off
Tear faults
Ionian subduction system

ABSTRACT

The Ionian subduction in the central Mediterranean, just 200 km wide, is one of the narrowest in the world. Its evolution has involved a progressive disruption of the subducting slab, contemporaneous to the retreat and step-wise opening of back-arc basins. In this study, we analyse velocity anomalies of the upper mantle, together with the most comprehensive set of earthquake locations and kinematic indicators available for Italy, to reconstruct the geodynamics and tectonic evolution of the Ionian subduction system. Along the Sicilian boundary, we identify an eastward migration of the slab edge with detachment of the Ionian oceanic lithosphere. We hypothesize that the progressive detachment of the slab took place along lithospheric transform faults of the Neo-Tethys Ocean. Among the main active kinematic elements of the Ionian accretionary wedge, we suggest that a ∼400-km-long and highly segmented shear zone formed by the Aeolian-Tindari-Letojanni fault system and the Ionian fault represents the surface expression of such a lithospheric tearing. The present day convergence between the Eurasian and African plates is accommodated both at the frontal thrust of the flexed Hyblean margin in southern Sicily and offshore along the Tyrrhenian Sea. Lithospheric bending favors the wedging of the mantle underneath northern Sicily, while magmatic fluids are channeled along slab tears.

1. Introduction

Progressive slab migration and lithospheric tearing have been observed at a number of retreating subduction zones (see Wortel et al., 2009 and references therein). These processes lead to a progressive segmentation of the subduction zone, giving rise to complex geodynamic settings. The mechanism of segmentation depends on several factors such as i) the rollback rate variations along the strike of the subduction system, and ii) the lithospheric structures, thickness and strength. Furthermore, the geodynamic setting may be even more complex owing to the presence of pre-existing lithospheric discontinuities that can be reactivated to accommodate the deformation related to the subduction process. The central Mediterranean region seems an ideal template for understanding these processes.

The active tectonics in the central Mediterranean is the result of different processes that followed the closure of Mesozoic oceans (Dercourt et al., 1986; Dewey et al., 1989), the collision between the Eurasia and Africa plates and the post-collisional collapse of the Apennine belt, along with the simultaneous subduction-retreat of the Ionian lithosphere (Malinverno and Ryan, 1986; Anderson and Jackson, 1987; Doglioni, 1991; Faccenna et al., 2001). In such a tectonic puzzle, earthquake hypocenters alone cannot provide evidence for a simple boundary between major plates but are rather distributed in a broader zone along the continental lithosphere (Fig. 1). Such a complexity is also recognized by the GPS-based crustal velocity map (Fig. 1; see Appendix A for details), which is characterized by velocity gradients related to tectonic interactions between minor crustal blocks.

Here, we focus on active tectonics along the southern Tyrrhenian plate boundary, resulting from poly-phased episodes of oceanic subduction, slab retreat, and continental collision (Dewey et al., 1989; Faccenna et al., 2001). The evolution of this plate boundary is dominated by the subduction of the Ionian lithosphere, a terminal branch of the Permo-Triassic Neo-Tethys Ocean (Stampfli, 2000). A broad spectrum of observations, spanning from the distribution of seismicity to tomographic anomalies, receiver functions and SKS splitting, supports the suggestion that the Ionian slab progressively retreated south-eastward, together with the opening of the back-arc basins in the Tyrrhenian sea and the drift of the Calabrian Arc (Anderson and Jackson, 1987; Selvaggi and Chiarabba, 1995; Faccenna et al., 2001; Lucente et al., 2006; Giacomuzzi et al.,

* Corresponding author.
E-mail address: mimmo.palano@ingv.it (M. Palano).

http://dx.doi.org/10.1016/j.jog.2017.01.006
0264-3707/

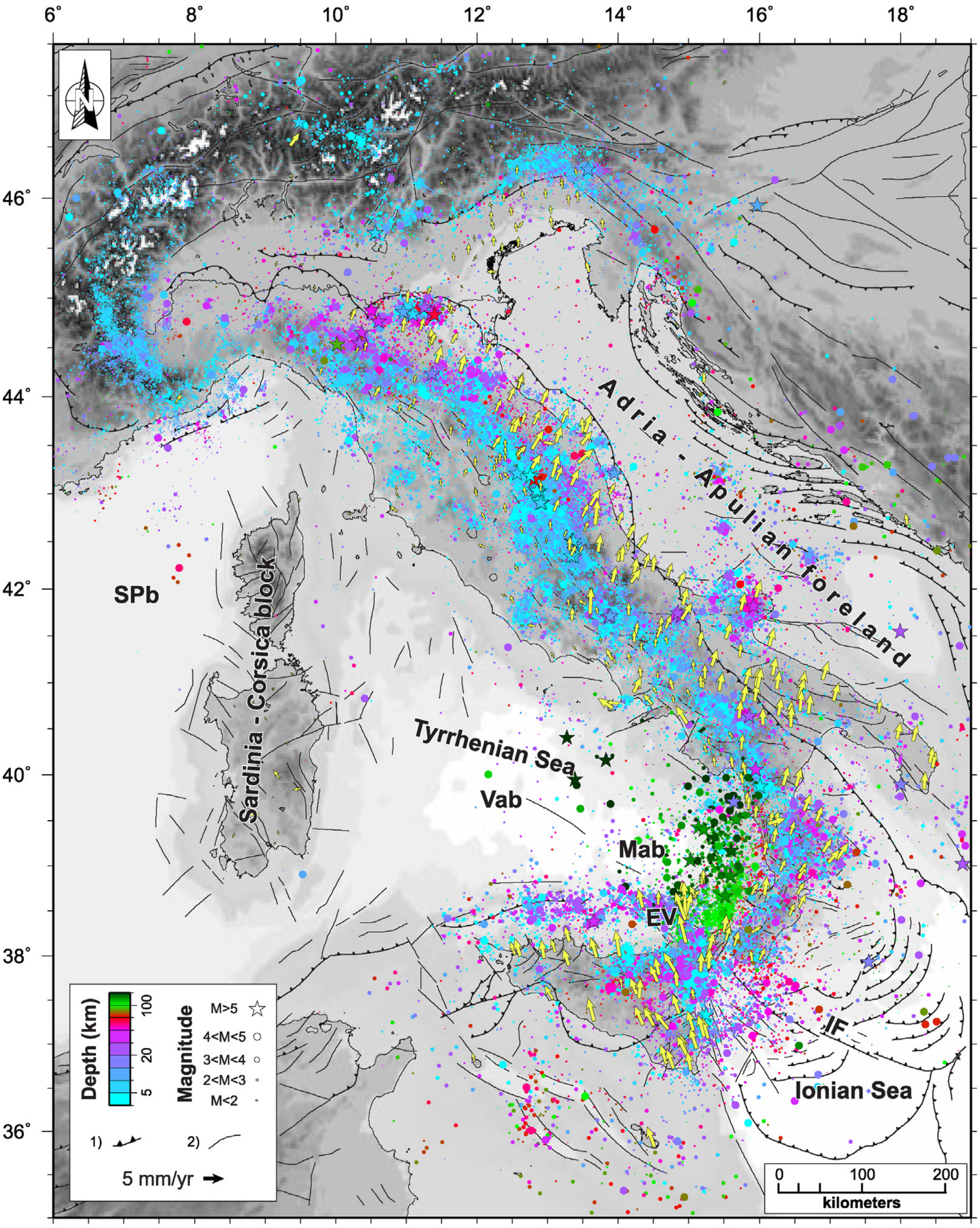

Fig. 1. Instrumental seismicity occurring from 1981 up to 2013 along the Italian Peninsula (Chiarabba et al., 2005, 2015; Castello et al., 2006). Earthquakes are colored as a function of the focus depth, while different symbols indicate the magnitude range. The GPS-based velocity field (yellow arrows) in a fixed Eurasian reference frame is also reported. Abbreviations: EV, Aeolian Volcanoes; Mab Marsili basin; Vab, Vavilov basin; IF, Ionian fault; SPb, Sardinia-Provençal basin. (For interpretation of the references to colour in this figure legend, the reader is referred to the web version of this article.)

2012). Kinematic indicators and geodynamic models indicate that the Africa-Eurasia oblique convergence is currently occurring at a rate of ∼7–8 mm/yr (e.g. DeMets et al., 2010; Nocquet and Calais, 2003). The plate boundary along which this convergence is accommodated is fragmented and the deformation is distributed broadly over large portions of the continental lithosphere (e.g. Palano et al., 2012 and references therein). Part of the compressional deformation is absorbed offshore of northern Sicily, where seismicity and focal mechanisms reveal a broadly E-W trending thrust belt (e.g. Billi et al., 2007). The complex geodynamic processes are also evidenced by the broad extension observed in northern Sicily (Billi et al., 2010; Palano et al., 2012), along a coast-parallel mountain range where historical moderate earthquakes, associated with prevailing normal faulting, occurred (Rovida et al., 2011).

In this study, we provide additional constraints on the lateral progressive change along the plate boundary, from subduction to slab break-off and subsequent flexuring of the Sicilian continental margin. We use the most complete set of accurately located seismicity and GPS data to build an improved picture of the current tectonic setting of the plate boundary. We integrate this information with tomographic images of the mantle that fix the location and geometry of the subducted Ionian lithosphere, enabling to resolve the evolution of the entire subduction system since about 30 Ma. Finally, our findings are framed in the general geodynamic setting of the central Mediterranean region by also taking into account recent geological and geophysical observations.

2. Background setting

Subduction and back-arc extension in the central Mediterranean started ∼30 Ma (Faccenna et al., 2014 and references therein). These processes were responsible for i) crustal thinning and the opening of the Liguro-Provençal basin, ii) growth of a volcanic arc along the Sardinia-Provençal margins (Beccaluva et al., 2005; Lustrino et al., 2000) and iii) ∼40° counterclockwise rotation of the Sardinian-Corsica block (Gattacceca and Speranza, 2002). This phase of subduction rollback and back-arc extension was active at least until 16 Ma (Speranza et al., 2002 and references therein) and terminated by the collision with the Adria-Apulian microplate and the formation of the Apennine orogenic system (Patacca et al., 1990).

After a period of quiescence, in the early Tortonian (∼12-10 Ma) the Tyrrhenian basin started to open in response to the southeastern rollback of the northwestern subducting Ionian lithosphere. The first stage of Tyrrhenian opening (from ∼12-9 Ma up to 6-5 Ma), was characterized by widespread extension in the northern domain, and rifting in the western part of the southern domain (Rosenbaum and Lister, 2004). The magmatic arc migrated SE-ward from the Sardinia margin, where calcalkaline suites erupted during ∼15-13 Ma (Savelli, 2002), to the southern Tyrrhenian basin at 6-4 Ma (Vavilov basin) and at 2-1 Ma (Marsili basin), marking a second stage of opening, localized in the southern Tyrrhenian area. This new, faster, opening phase was characterized by subduction and rollback with rates as fast as 50–80 mm/yr (Patacca et al., 1990; Faccenna et al., 2001). The increase in rates of subduction rollback and back-arc spreading was probably favored by the formation of tear faults (Wortel et al., 2009) at the edge of the subducting slab. During this process, the margins of the Neo-Tethys underwent intense rotations (Gattacceca and Speranza, 2002; Mattei et al., 2007) with the accretion and stacking of sedimentary units in the Apennine-Maghrebian orogenic system (D'Argenio et al., 1973; Casero et al., 1988).

Since the Middle Pleistocene, when the magmatic arc reached its present-day position in the Aeolian Islands, both the back-arc Tyrrhenian extension and the rollback of the subducting Ionian lithosphere ceased or significantly slowed (e.g. Faccenna et al., 2001; Wortel and Spakman, 2000; Goes et al., 2004; Palano et al., 2017).

The NW-dipping Ionian slab is clearly recognized beneath the allochthonous Calabrian Arc by tomographic images and deep earthquakes (Chiarabba et al., 2008; Calò et al., 2013; Neri et al., 2009; Giacomuzzi et al., 2012). Multichannel seismic profiles of the Ionian accretionary wedge (e.g. Cernobori et al., 1996; Minelli and Faccenna, 2010; Gallais et al., 2013; Polonia et al., 2011) show a pile of sediments scraped off from the slab and piled up along thrust faults, resulting in the emplacement of a thick (up to 10 km) and ∼200–300 km wide complex. Recently, a NW-SE-striking fault system (hereinafter Ionian fault; Fig. 1), was proposed as separating the Ionian accretionary wedge into two main lobes (Polonia et al., 2011). However, the kinematics of this fault is debated, with authors proposing either dextral strike-slip features along its entire length (e.g. Polonia et al., 2016 and references therein) or left strike-slip motions along its southeastern sector (Gutscher et al., 2017).

3. Seismological and geodetic data

To improve the resolution of the crustal tectonic features of the investigated area, as well as to highlight the main structure of crust and upper mantle, we used an updated dataset of seismic observations. A complete dataset of seismicity was obtained by merging the CSI catalog (period 1981–2002: Chiarabba et al., 2005; Castello et al., 2006) with its consistent update to 2013 recently reported in Chiarabba et al. (2015). For the study area, the entire set of locations consists of about 137,000 crustal earthquakes, with hypocentral errors within 2 km, and 3013 deep earthquakes (Fig. 2). In addition, numerous tomographic studies have investigated the southern Tyrrhenian region, highlighting the structure of the crust

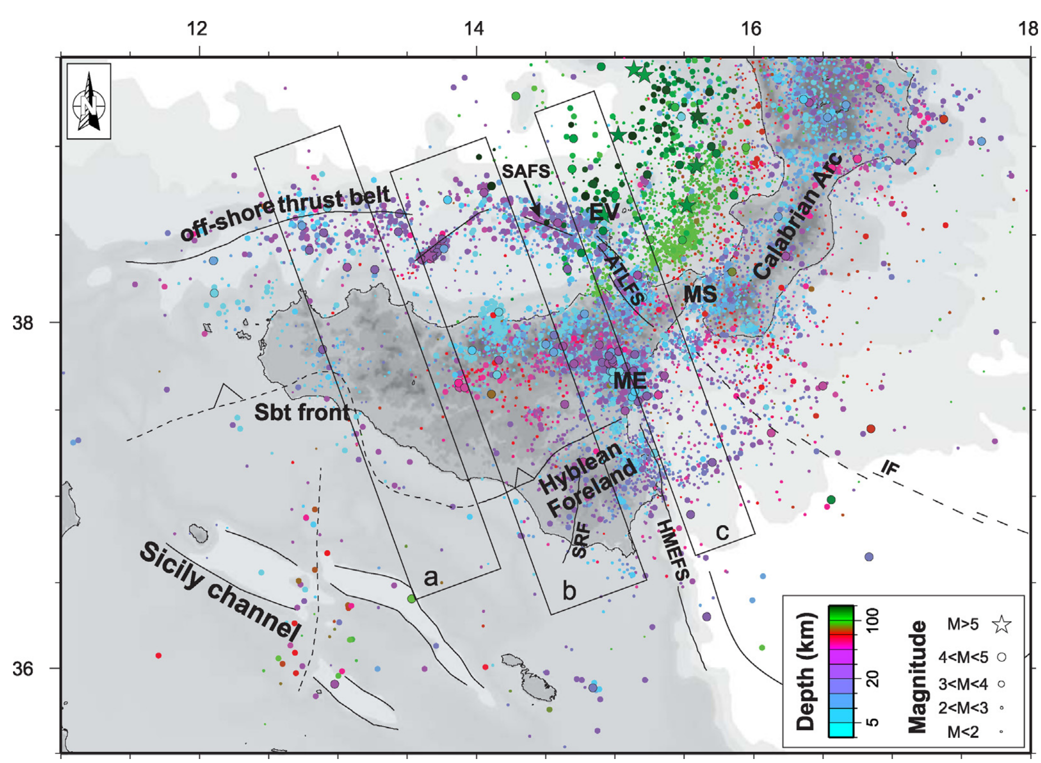

Fig. 2. Simplified tectonic map of the Sicilian-Calabrian area. Earthquake symbols and colors are as Fig. 1. Boxes a–c show the events reported as vertical sections in Fig. 3. Abbreviations: SAFS, Sisifo-Alicudi fault system; ATLFS, Aeolian-Tindari-Letojanni fault system; HMEFS, Hyblean-Maltese Escarpment fault system; EV, Aeolian Volcanoes; ME, Mount Etna; MS, Messina Strait; IF, Ionian fault; SRF, Scicli-Ragusa fault.

and upper mantle with different depth penetration and resolution (Selvaggi and Chiarabba, 1995; Lucente et al., 1999; Wortel and Spakman, 2000; Piromallo and Morelli, 2003; Chiarabba et al., 2008; Giacomuzzi et al., 2011; Calò et al., 2013). In this study, we use the high resolution S-wave velocity model obtained recently by Giacomuzzi et al. (2012), because S-wave and V_P/V_S values together enable discerning between compositional and thermal effects in the generation of velocity anomalies in the mantle.

In addition, we analysed an extensive GPS dataset spanning the 1994.0–2015.4 time interval and covering the whole Italian peninsula (see the see Appendix A for details about GPS networks and data processing).

3.1. Crustal seismicity

Over the investigated area, the crustal seismicity is distributed along i) the offshore of northern Sicily, ii) in eastern Sicily and its associated offshore area and iii) along the whole Calabrian Arc (Fig. 2). Along the Sicilian border of the subduction/collision system, such a distribution shows a remarkable lateral change (Fig. 2). In western Sicily, earthquakes are few and sparse and mainly concentrated along the northern offshore associated with a broad E-W trending compressional system with an en-echelon faults arrangement. Such a compressional system follows the positive structures of the submarine plateau, almost parallel to the Tyrrhenian coast, and appears seismically connected with the faults located along the western sector of Aeolian Islands (Fig. 2). Seismicity remains confined above the depth of 35 km (Fig. 3a) and does not show bending of the continental lithosphere that seems almost flat as the compressional system in the offshore of northern Sicily.

Eastward, excluding the dense cloud of earthquakes located in the Mt. Etna volcanic area, seismicity is mainly aligned along the western and central sectors of the Aeolian Islands and along the northern coastal area of Sicily. The former area is characterized by the presence of the Sisifo-Alicudi fault (a WNW-ESE oriented dextral strike-slip shear zone passing through the western sector of the Aeolian Islands; Fig. 2) and the Aeolian-Tindari-Letojanni fault system (a complex and heterogeneous crustal right-lateral shear zone consisting of a broad NNW-SSE- to NW-SE-trending system of faults running from the central sector of the Aeolian Islands down to the Ionian offshore of Sicily; see also Palano et al., 2015 for additional details). The latter area corresponds to a domain subject to a prevailing N-S crustal stretching as indicated by earthquake fault-plane solutions (Pondrelli et al., 2004; Palano, 2015), GPS observations (Palano et al., 2012) and Quaternary geostructural data (e.g. Billi et al., 2010 and references therein). In both areas, seismicity appears confined above the depth of 35 km.

In central and eastern Sicily, seismicity is intense and diffuse (Fig. 2). In particular, seismicity on the Hyblean foreland is distributed on its eastern sector, close to the Hyblean-Maltese Escarpment fault system (Fig. 2; a Mesozoic lithospheric boundary separating the Sicilian continental crust from the Ionian oceanic basin; e.g. Palano et al., 2012) and along the Scicli-Ragusa fault (Fig. 2; a left-lateral N-S oriented shear zone separating the Hyblean foreland into two different tectonic crustal blocks; e.g. Musumeci et al., 2014) and is mainly confined to the 10–25 km depth interval (Fig. 3b). Northward, seismicity deepens down to 60–70 km, expressing the bending of the Hyblean continental lithosphere beneath the thrust nappes of the mountain belt. Fig. 3c shows similar features to those reported in Fig. 3b, with the exception of intermediate depth earthquakes occurring down to 100 km, which define a steeply NW-dipping structure.

The Ionian offshore area of eastern Sicily and southern Calabria, including the Messina Strait and the lobes of the accretional wedge, is characterized by sparse seismicity with shallow hypocenters (Fig. 2). The poor resolution of hypocentral depths does not allow associating these earthquakes to the lower plate boundary, but the best-located events mostly occur in the Ionian lithosphere and do not cluster on specific sub-horizontal decollements. In addition, deeper earthquakes are confined to the eastern lobe (eastward from the Ionian fault), while in the western lobe they are mainly confined above depths of 30 km (Fig. 2). Moreover, the Ionian fault appears seismically connected with the Aeolian-Tindari-Letojanni fault system as evidenced by a near-continuous NW-trending corridor of abundant seismicity running from the central sector of the Aeolian Islands down to the Ionian offshore of Sicily (see also Palano et al., 2015 for additional details).

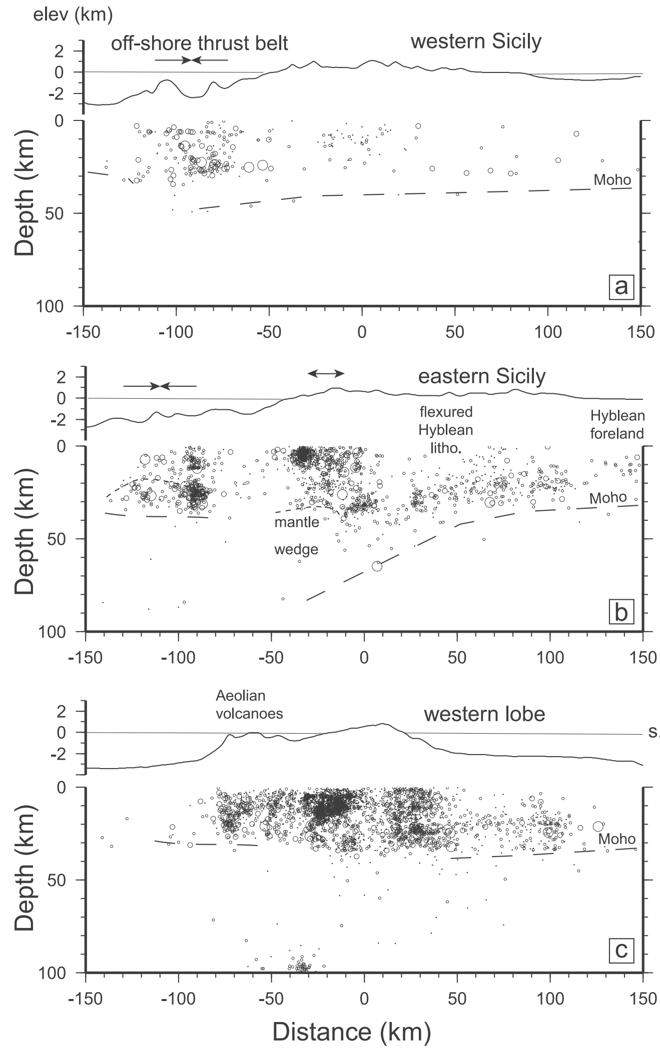

Fig. 3. Vertical sections of seismicity distribution. Earthquakes are classified according to the magnitude range.

3.2. Deep and intermediate depth seismicity

Deep and intermediate earthquakes are mainly located in the Tyrrhenian side of the Calabrian Arc clearly defining the steep NW-dipping Ionian subducting slab (Fig. 4a). The slab appears seismically continuous down to a depth of ~350 km, and is characterized by the occurrence of several earthquakes with magnitude $M \geq 5$ along its deeper portion (Fig. 4b). The distribution of deep and intermediate depth earthquakes shows evidence of two vertical boundaries along the subduction system with a progressive fading of deep events proceeding westward from the Ionian subduction (Figs. 2 and 4). The first transition is a marked boundary at the

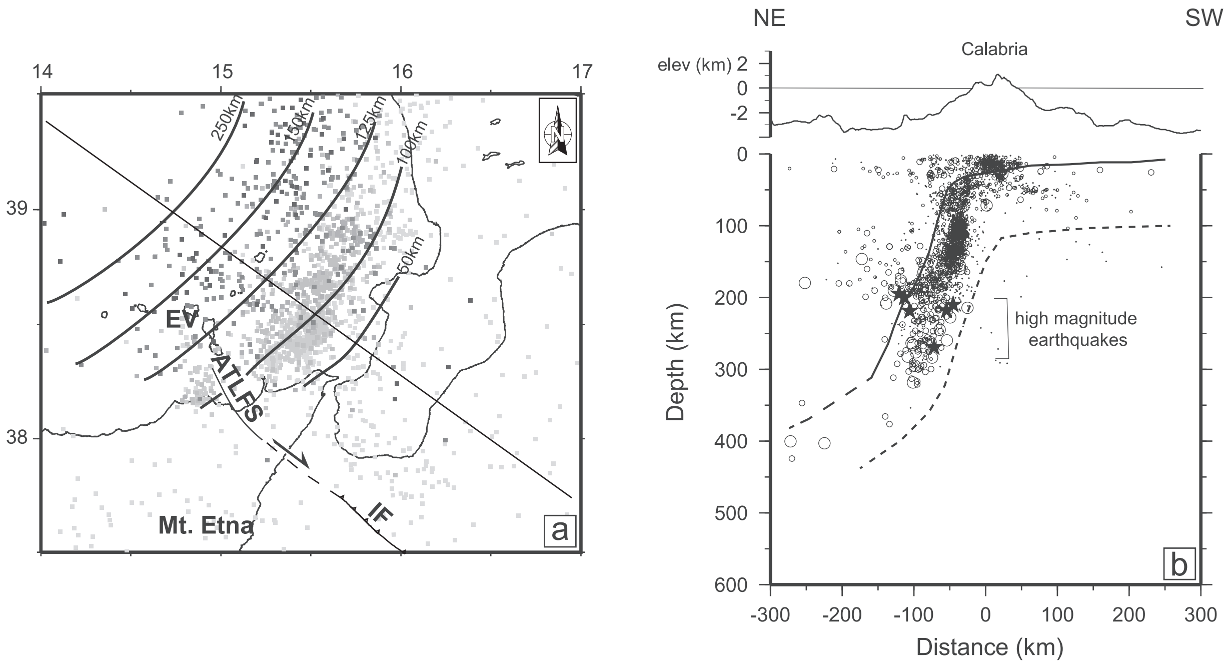

Fig. 4. a) Deep and intermediate seismicity located beneath the Calabrian Arc; the contour defines the NW-dipping Ionian subducting slab as depicted by the depth distribution of seismicity. Abbreviations: ATLFS, Aeolian-Tindari-Letojanni fault system; IF, Ionian fault. The connection between ATLFS and IF is redrawn from Palano et al. (2015). b) Vertical section across the Calabrian Arc region; earthquakes are classified according to the magnitude range.

western terminus of the Ionian subducting slab, where deep earthquakes abruptly vanish to the west of the Aeolian Islands. Indeed, a rarefying of the slab-related seismicity can be observed below the central sector of Aeolian Islands, along a NW-trending corridor that follows the crustal trace of the Aeolian-Tindari Letojanni fault system (Fig. 4a).

The second transition can be identified by the different distribution of intermediate-depth earthquakes between the central and western sectors of Sicily. In the former, earthquakes occur down to a depth of ~80–100 km (Fig. 3b) and are related to the northward flexure of the Hyblean lithosphere; in the latter, intermediate-depths earthquakes are absent (Fig. 3a). At shallow depth, such a transition clearly marks the cessation of seismicity along the northern coastal area of Sicily, at the longitude of ~13.5°E (Fig. 2).

The updated seismic catalog also reveals a broadly N-S elongated strip of seismicity in the Sicily channel offshore (Fig. 2). Although the current geometry of the seismic network on this area only permits locate magnitude ≥ 3.0 earthquakes, such a strip of deep seismicity marks the N-S segmentation of the extensional Sicily channel system into two separate branches.

3.3. *Crustal and mantle tomography*

In this study, we use the high-resolution S-wave velocity model recently obtained by Giacomuzzi et al. (2012). This velocity model has a spatial resolution in the order of tens of kilometers for the whole upper mantle, allowing outlining the slab geometry with unprecedented details. Such a high-resolution tomography has revealed a continuous high V_S NW-ward dipping volume (i.e. the subducting Ionian lithosphere; Fig. 5), which extends from the surface (beneath the Calabrian Arc) to the mantle transition zone (beneath Sardinia). Based on the geometry of deep velocity anomalies, coupled with paleogeographic records of the subduction process (e.g. Faccenna et al., 2014 and references therein), we provide additional constraints on the subduction history. In the following, two main stages are considered, before and after the opening of the southern Tyrrhenian oceanic basin respectively.

3.3.1. *First stage of subduction <18-6 Ma*

During the first episode, a narrow oceanic corridor was slowly subducting beneath Sardinia. The remnants of the oceanic lithosphere subducted during this episode are well defined by positive V_S anomalies between 520 and 360 km depth (Fig. 5). The overall geometry of remnants in the mantle fits the retreat of the slab, whose eastward route is defined by SKS splitting in the mantle (Lucente et al., 2006). Seismicity does not currently occur within these old oceanic remnants, which are dived in the upper mantle.

3.3.2. *Second stage of subduction 6-5 Ma to present*

The most recent episode of subduction took place entirely in the southern Tyrrhenian area, with fast subduction and rollback of the oceanic lithosphere (Rosenbaum and Lister, 2004), associated with ultra-fast opening of the oceanic basins (Nicolosi et al., 2006). Mantle V_S anomalies located between 220 and 100 km depth describe the vertical geometry of the steep slab (Fig. 5). The visual inspection of the horizontal extension of these V_S anomalies at different depth levels, highlights how the main V_S anomaly is mainly located in the Tyrrhenian offshore of Calabria. Moreover, a progressive eastward propagation of the south-western slab edge can be inferred from the distribution of the high V_S anomalies along the northern Sicilian offshore at the depths of 220 km (Fig. 6a) and 100 km (Fig. 6b). In fact, the shift between the position of the high V_S perturbation between the 220 km and 100 km depth slices lends weight to the eastward migration of the south-western slab tear. The south-western slab edge is marked in Fig. 6 as a black dashed line roughly bounding the lateral extent of the high V_S anomalies along the northern Sicilian offshore. Such a line is reported with a ~N130E° orientation, however, a wider range of possible orientations could be considered.

The vertical sections across the western terminal part of the slab visualize details of a progressive detachment of the oceanic lithosphere, with different maturation from west to east (Fig. 6c). Deep earthquakes still occur within the high velocity slab recently detached beneath the western lobe of the Ionian accretionary wedge (Fig. 3c) but not in eastern Sicily where the process is

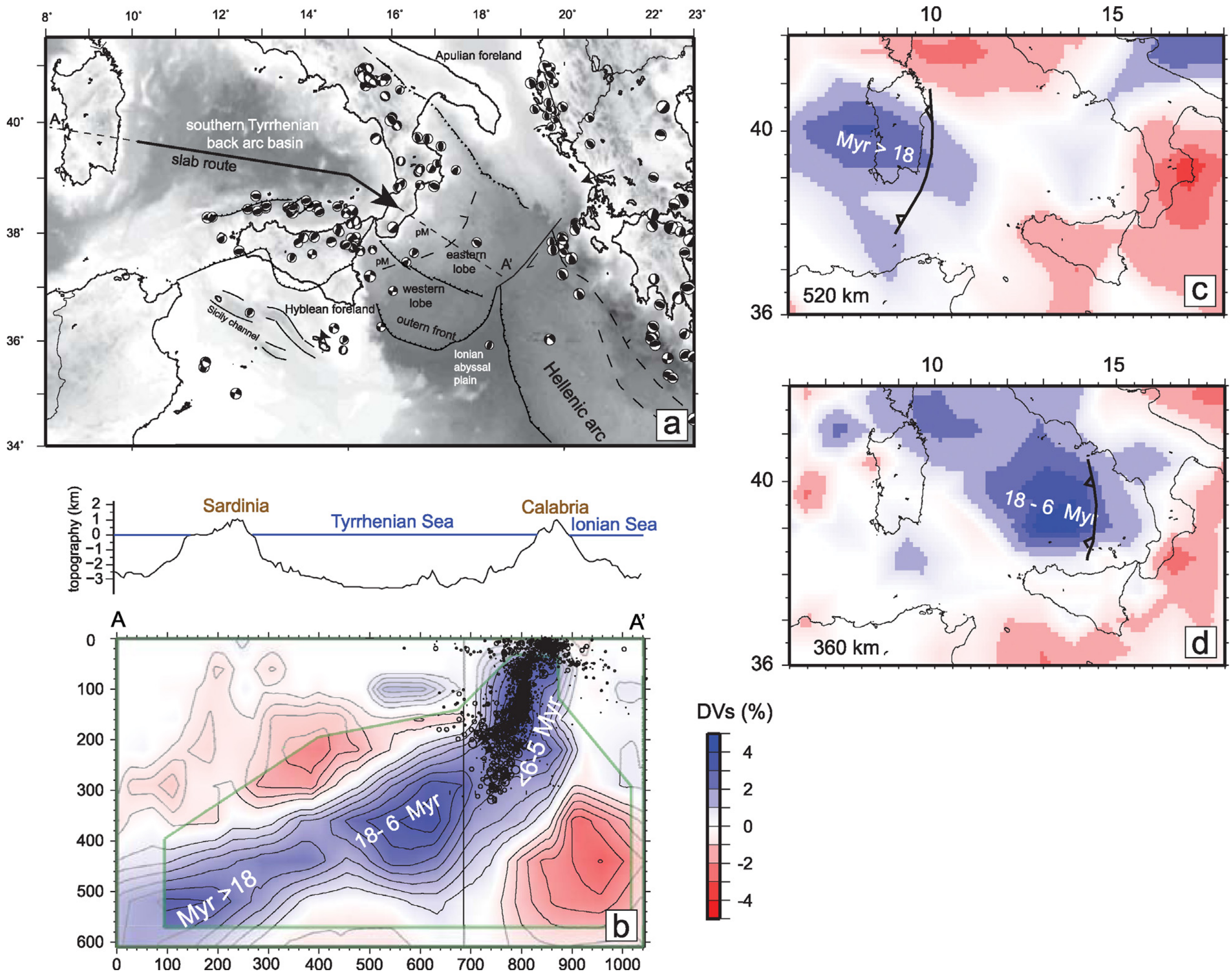

Fig. 5. a) Sketch map of central Mediterranean showing the eastward migration of the Calabrian subduction system. The route of the Calabrian subduction system follows approximately the direction of maximum back-arc extension, according to Faccenna et al. (2001). Focal mechanisms of earthquakes with magnitude $M \geq 4$ are also reported (www.globalcmt.org). b) Vertical section across the Tyrrhenian Sea showing the V_S velocity anomalies. Map views of V_S velocity anomalies at depth of 520 km (c) and 360 km (d). Ages refer to different stages of the subduction process.

older (Figs. 2 and 3c). Moreover, beneath the eastern lobe of the accretionary wedge, the slab appears continuous as evidenced by the high V_S anomaly and the occurrence of abundant earthquakes down to a depth of ~350 km (Fig. 4b).

3.4. GPS data

The GPS-based velocity field for the entire Italian peninsula aligned to a fixed Eurasian reference frame (Cannavò and Palano, 2016) is reported in Fig. 1. To highlight the crustal deformation pattern over the study region, we computed the 2-D strain-rate tensor following the strategy reported in Palano (2015). The estimated strain-rates are reported in Fig. 7: the arrows show the greatest extensional ($\varepsilon_{\mathrm{Hmax}}$) and contractional ($\varepsilon_{\mathrm{hmin}}$) horizontal strain-rates, respectively. The strain-rates map allows identifying four main domains characterized by different deformation pattern. Along the Tyrrhenian offshore of Sicily (i.e. from Ustica to the Aeolian Islands), the strain-rate pattern is predominantly contractional with ε_{hmin} axes having orientations ranging from NW-SE to N-S with values up to 70 nanostrain/yr. A large sector of north-central Sicily is characterized by crustal stretching with ε_{Hmax} axes oriented from N-S to NNE-SSW with values up to 30 nanostrain/yr. In the north-eastern corner of Sicily and southern Calabria, the strain-rate pattern is predominantly extensional with ε_{Hmax} axes prevailing oriented along the WNW-ESE attitude with values up to 65 nanostrain/yr. The southern sector of Central Sicily, comprising also the north-western Hyblean foreland, is characterized by crustal shortening with ε_{hmin} axes having values up to 40 nanostrain/yr.

4. Discussion

Deep earthquakes and tomographic images yield tracing both the location and geometry of the subducted Ionian lithosphere, providing additional constraints on the subduction history during the past 30 Ma. Previous reconstructions of the central Mediterranean were done on the basis of large-scale P-wave velocity models computed with variety of data and techniques (Lucente et al., 1999; Wortel and Spakman, 2000; Piromallo and Morelli, 2003) and include models of slab retreat (Faccenna et al., 2001; Rosenbaum et al., 2002), slab detachment, slab tearing (Chiarabba et al., 2008; Neri et al., 2012), lithospheric delamination (Chiarabba and Chiodini, 2013) and dynamic topography sustained by mantle flow (Faccenna and Becker, 2010). Although P-wave anomalies in the upper mantle are generally assumed to reflect thermal difference, recent high resolution models of the area (Giacomuzzi et al., 2012) demonstrated that V_S and V_P/V_S models are more effective to discriminate between thermal and compositional effects and to give a direct image of the anomalies related to the cold slab. High

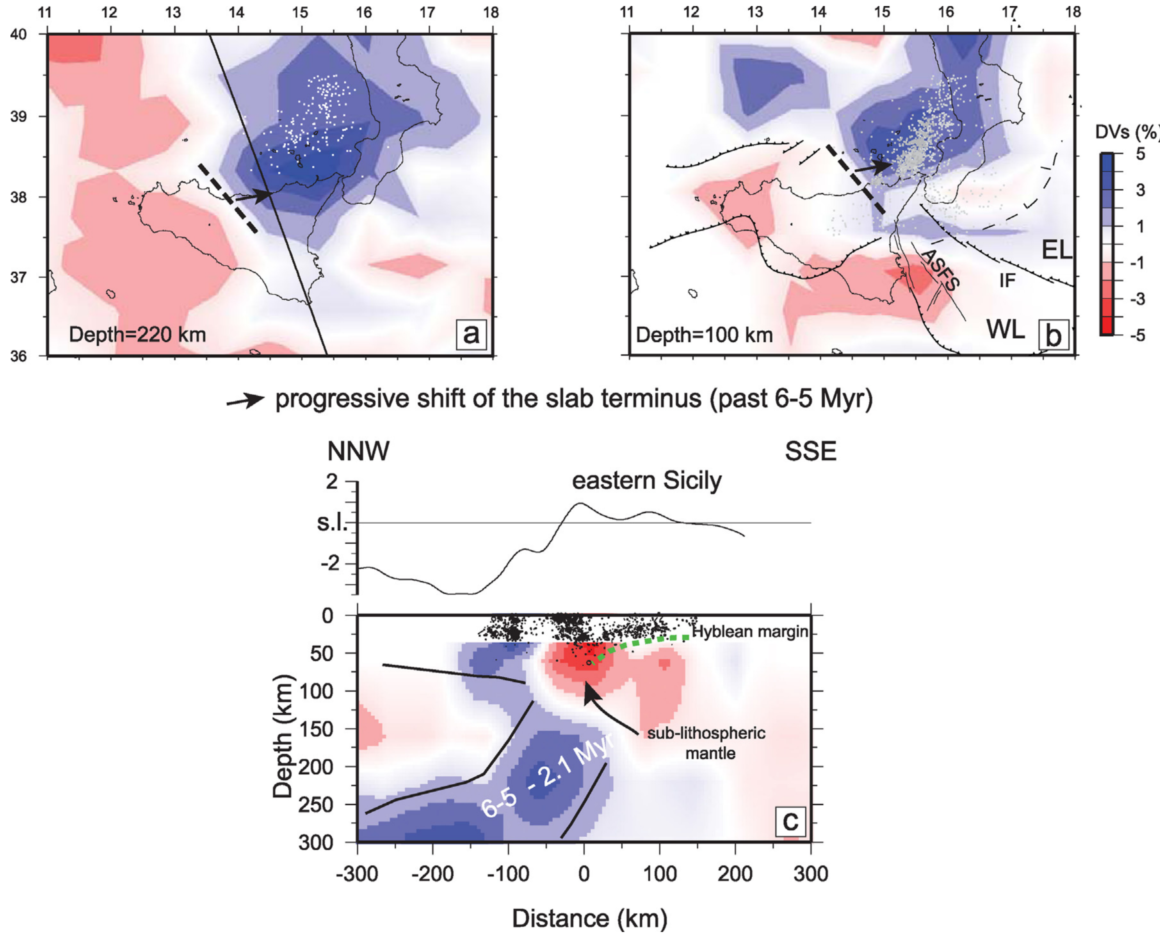

Fig. 6. Schematic maps showing the progressive migration of the western edge of the slab in the last 6-5 Myr (upper panels). Vertical section across central (a) and eastern (b) Sicily showing the distribution of V_S velocity anomalies. Abbreviations: IF, Ionian fault; ASFS, Alfeo Seamount fault system (Gutscher et al., 2016).

V_S anomalies at 520 and 360 km depth (Fig. 5) delineate the extent of the subducted Neo-Tethys Ocean, consistent with the long route travelled by the slab during the retreat (Malinverno and Ryan, 1986; Lucente et al., 2006). With respect to previous reconstructions, the westward subduction was limited to a narrow area, where Sardinia served as the foreland. Orogenic magmatism occurred along the western margin of Sardinia during a relatively long period (from ∼38 to ∼12 Ma), even though most of the activity was concentrated around ∼21-18 Ma (Lustrino et al., 2011). In Early Tortonian (∼12-10 Ma), the Ionian slab (as previously defined, the terminal branch of the Permo-Triassic Neo-Tethys ocean) started to retreat, leading to the SE-ward migration of the magmatic arc from the western Sardinia margin to the Tyrrhenian basin (15-13 Ma; Savelli, 2002). The slab subducted during the 18-6 Ma time interval lies beneath the central Tyrrhenian basin and is located in the depth interval of 360–220 km, as suggested by high V_S anomalies (Fig. 5).

After a quiescent period, in early Pleistocene, activity resumed in the southern Tyrrhenian area with very fast subduction and slab rollover (e.g. Faccenna et al., 2001, 2014). The geometry of the subducted slab is well documented by anomalies in the uppermost mantle. High V_S in the depth range between 220 and 100 km (Fig. 6) shows a progressive decrease in the lateral extent of the subducted oceanic lithosphere, suggesting a progressive slab detachment (and subsequently sinking in the mantle) along the northern Sicilian offshore area. In particular, along this area, the south-western slab edge migrated ∼100 km eastward after the Lower Pliocene. The progressive slab detachment and eastward migration is also confirmed by anisotropy in the upper mantle, which shows a pattern consistent with a mantle return flow through a tear at the south-western edge of the slab (see Baccheschi et al., 2011 and references therein). In addition, we hypothesize that an E-W-elongated anisotropy observed beneath inland Sicily (Baccheschi et al., 2011) records the upper mantle flow originating during the progressive eastward migration of the subduction zone.

At the lithospheric scale, such a progressive migration was accommodated by the development of a wider W-E trending right-lateral shear zone, characterized by both a synthetic NW-SE/W-E oriented, and antithetic left-lateral N-S/NE-SW fault systems, which on dissecting the Maghrebian chain, have over time migrated eastward (Finetti and Del Ben, 1996; Giunta et al., 2009). The development of these fault systems corresponds to a spatial and temporal progression from active subduction to slab detachment and recently, to the onset of compression. In this framework, western Sicily was located at the edge of the subduction and underwent intense rotations during the entire subduction process (Mattei et al., 2007). The subducting lithosphere tracked by high velocity bodies along with seismicity and kinematic indicators enable resolving how the fault systems/discontinuity have evolved over time.

The first and older discontinuity, approximately NNW-SSE oriented, is located in central Sicily and likely represented the western slab boundary during the entire Pliocene, when subduction continued east of the discontinuity, with the flexure of the Hyblean lithosphere and sedimentation in thrust-top and foredeep basins. According to the age of the sedimentary sequences, the process ended in the Upper Pliocene – Early Pleistocene (Casero, 2004). In agreement, geological, gravimetric, and seismic data provide

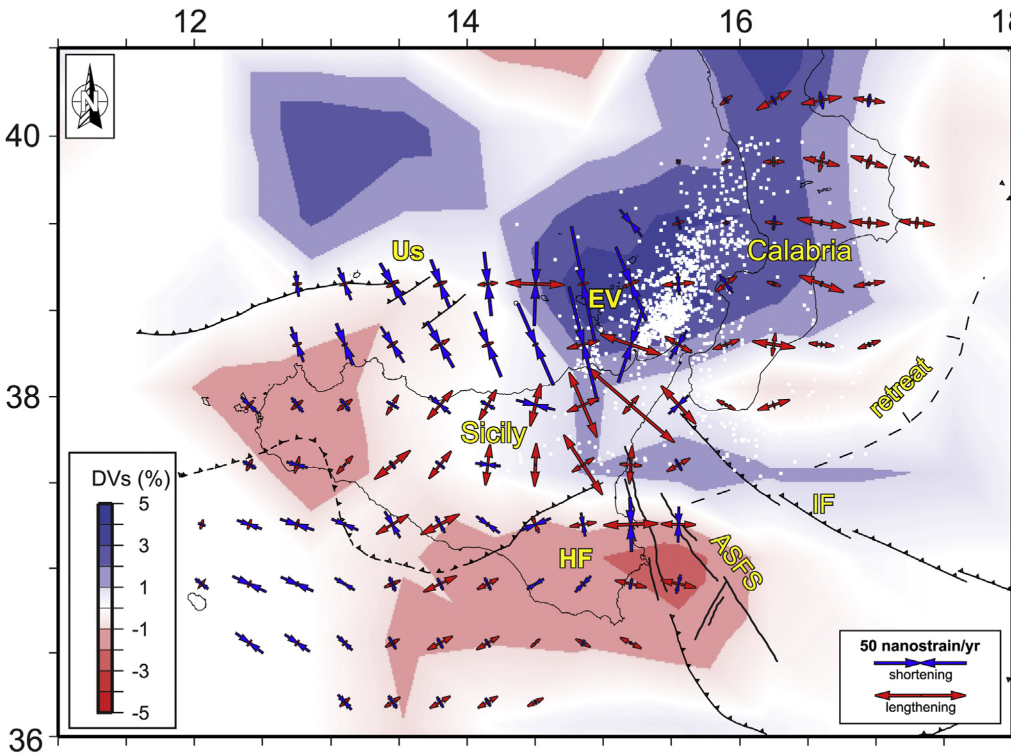

Fig. 7. Geodetic strain-rates: arrows represent the greatest extensional (red) and contractional (blue) horizontal strain-rates. The distribution of V_S velocity anomalies at the depth of 100 km are also reported. Abbreviations: IF, Ionian Fault; ASFS, Alfeo Seamount fault system; Us, Ustica; EV, Aeolian Volcanoes; HF, Hyblean foreland. (For interpretation of the references to colour in this figure legend, the reader is referred to the web version of this article.)

evidence for a 100-km-long, NW-SE oriented shear zone in central-eastern Sicily, interpreted as a lithospheric-scale structure serving as a step fault since the Pliocene – Early Pleistocene (Barreca et al., 2016). The location of this step fault matches well the limit of the high V_S anomaly at 220 km depth, giving a strong constraint to the position of the Pliocene slab boundary. Indeed, such a step fault might be interpreted as the surface expression of the old lateral slab tearing discontinuity.

The second discontinuity coincides with the slab edge at 100 km depth (early Quaternary subduction), and is defined by a NNW-trending lineament continuing further south, with a set of lithospheric structures cutting the offshore of eastern Sicily. The Hyblean-Maltese Escarpment fault system represents the westernmost structure of this set. A number of studies have reported active normal faulting on the northern portion of this fault system (e.g. Argnani et al., 2012). The easternmost structure, recently discovered by high-resolution bathymetry and seismic profiling (see Gutscher et al., 2016, 2017 and references therein) is represented by a 140 km long, two-branched fault system (ASFS; Fig. 7) running eastward of the Alfeo Seamount up to Mount Etna where it merges with the dextral strike-slip faults cutting the SE flank of the volcano. This two-part fault is characterized by transtensional (normal and right-lateral strike-slip) faulting.

All these structures, including the Aeolian-Tindari-Letojanni and the Ionian faults, have been proposed, though within the framework of competing tectonic models, as a possible candidate for the shallow expression of a “STEP” (subduction tear edge propagator) fault (Govers and Wortel, 2005; Rosenbaum et al., 2008; Argnani et al., 2012; Gallais et al., 2013; Palano et al., 2015; Polonia et al., 2016; Gutscher et al., 2016, 2017). Based on available plate kinematic reconstructions, the southeastern Tyrrhenian Sea formed primarily during the Pleistocene, with a rapid southeastward migration of the Calabrian Arc (Faccenna et al., 2001, 2014; Rosenbaum and Lister, 2004; Jolivet et al., 2006). Therefore, during early Pleistocene, slab detachment propagated beneath eastern Sicily and subduction continued in the Ionian basin. Major tearing of the subduction system occurred during this phase, with marked retreat of the Ionian trench. In this framework, the northern sector of the Hyblean-Maltese Escarpment fault system and ASFS likely represents, respectively, the oldest and the youngest tectonic expressions of the lateral slab tear fault during Pleistocene. Such a simplified reconstruction can explain the abrupt change in strike direction of compressional anticline fold axes east and west of ASFS (Gutscher et al., 2016), marking two different steps of the/a slab tearing process during the Pleistocene. We propose that in late Pleistocene the tearing process ceased in this area, while faults are currently accommodating part of the ongoing convergence, as testified by seismic and GPS data (Fig. 7). In addition, the destructive M > 7, 1169 and 1693 earthquakes probably originated in this area, although the causative faults are still unknown and debated (see Musumeci et al., 2014; Gutscher et al., 2016 for additional details).

The progressive decrease in the lateral extent of the subducting slab has been proposed as the cause of slowing or cessation of the rollback and subduction, and back-arc Tyrrhenian extension, started in Middle Pleistocene (e.g. Goes et al., 2004). This process may also have contributed to the decoupling of the Ionian subduction along discontinuities like the Ionian fault (Fig. 7), as indicated by the distribution of earthquakes within the slab and the southeastward motion (with respect to the foreland areas) of the Calabrian Arc (Palano et al., 2012). Based on seismological, structural and kinematic evidences, Palano et al. (2015) proposed that the Ionian fault, along with its inland continuation, the Aeolian-Tindari-Letojanni fault system, forms a ~400-km-long highly segmented crustal shear zone with prevailing right-lateral kinematics. The entire kinematic dataset confirms that this system, extending from the Aeolian Islands to the Ionian Abyssal plain, is the recent lateral slab tearing discontinuity (see also Palano et al., 2017). Along this system, only few deep earthquakes occur within the slab (Figs. 4 and 7), suggesting that tearing is ongoing along with channeling of magmatic fluids through the Aeolian volcanoes corridor. A similar relation between the development of tear faults and magmatism caused by upwelling of asthenospheric material has been suggested for Mt. Etna and Mt. Vulture volcanoes (see Rosenbaum et al., 2008 for an overview).

The evolution of the margin is at the basis of the lateral change of tectonics documented by GPS and seismicity between western and eastern Sicily. In this latter area, the presence of earthquakes highlights the current flexure of the Hyblean lithosphere, indicating its ongoing bending underneath the belt. This suggests that part of the compression is still accommodated across the eastern sector of the Sicilian frontal belt, paired with extension along the northern Tyrrhenian margin of Sicily that follows mantle wedging (Fig. 3). In western Sicily, the Africa-Eurasia convergence is primarily accommodated in the Tyrrhenian offshore in accordance with the absence of bending of the continental lithosphere.

The southern Tyrrhenian is an example of how segmentation of a plate boundary and progressive slab migration take place along inherited and newly formed lithospheric discontinuities. More generally, this study is relevant to other areas sharing tectonic similarities with the Ionian subduction system such as the Caribbean Sea (e.g. northeastern Caribbean), the western Pacific (e.g. Philippines, Indonesia, New Guinea), and the south Atlantic (Scotia arc).

5. Conclusive remarks

A large set of kinematic and seismic data, along with tomographic images of the upper mantle, yield a comprehensive picture of the subduction history of the southern Tyrrhenian slab and of active tectonics at the plate boundary. The evolution of the slab is conditioned by a progressive subduction of ancient lithospheric discontinuities created during the formation of the Ionian basin; the arrival of these ancient lithospheric discontinuities at the trench strongly segmented the subduction system. We derive some main conclusions on the tectonics of the area:

i) Along the southern Tyrrhenian plate boundary, we identify contiguous sectors with similar tectonic behavior bounded by lithospheric discontinuities. A main boundary exists between western and eastern Sicily as a response to the different evolution of the margin during subduction.
ii) In eastern Sicily, compression is still accommodated on the front thrust and along the flexed Hyblean margin, which first underwent lithospheric scale buckling in the Middle Pliocene paired with extension and uplift of the mantle wedge underneath the northern offshore of Sicily.
iii) In western Sicily, the continental lithosphere is not buckled and compression is concentrated further north as the Tyrrhenian offshore, near Ustica, 50 km offshore from the Tyrrhenian shoreline.
iv) The Ionian subduction is decoupled along a ~400-km-long highly segmented crustal shear zone. Including both the Aeolian-Tindari-Letojanni fault system and the Ionian fault, this likely represents the lithospheric expression of the tearing process affecting the retreating slab at least, since Middle Pleistocene. Such a shear zone, together with the Alfeo Seamount fault system, represent the main active kinematic elements of the Ionian accretionary wedge. These offshore segment faults are mechanically capable of generating magnitude 6–7 earthquakes and may be responsible for some enigmatic historical earthquakes (e.g. in 1908 in the Messina Strait and 1693 in eastern Sicily) that occurred in the area.

Acknowledgments

We thank the scientific and technical staff of INGV who continue to maintain the seismic network. We thank M.-A. Gutscher and an anonymous reviewer for their critical reviews and constructive comments that greatly improved the paper. We thank Stephen Conway for revising and improving the English language of this manuscript. We thank also Leica Geosystems S.P.A. (http://it.smartnet-eu.com), NetGEO (www.netgeo.it) Unavco facility (www.unavco.org), RGP (http://rgp.ign.fr), Regione Emilia Romagna (www.gpsemiliaromagna.it/), Regione Friuli-Venezia-Giulia (www.crs.inogs.it), Regione Calabria (http://gpscalabria.protezionecivilecalabria.it/), Regione Puglia (http://gps.sit.puglia.it), Regione Lombardia (www.gpslombardia.it/), Regione Abruzzo (http://gpsnet.regione.abruzzo.it/) for providing free access to GPS data.

Appendix A.

A.1 GNSS data Processing

Raw GPS observations were reduced to loosely constrained daily solutions by using the GAMIT/GLOBK software packages (Herring et al., 2010). The analysed dataset consists of 784 continuous GPS stations with more than 2.5 years of observations; these stations belong to various networks developed by a number of institutions and agencies for crustal deformation monitoring and commercial applications (mapping and cadastral purposes). To improve the overall configuration of the network and tie the regional measurements to an external global reference frame, data coming from more than 20 continuously operating global tracking stations, largely from the IGS (Dow et al., 2009) and EUREF (Beutler et al., 2008) permanent networks, were introduced in the processing. The loosely constrained daily GAMIT solutions were used as quasi observations in a Kalman filter (GLOBK) in order to estimate a consistent set of daily coordinates (i.e. time series) for all sites involved. Each time series was analysed for linear velocities, periodic signals (e.g. annual and semi-annual components) and antenna jumps by using the TSVIEW software package (Herring, 2003). In order to obtain clean time-series, any position estimate whose uncertainty was greater than 20 mm or whose value differed by more than 10 mm from the best-fitting linear trend was discarded. Then, we aggregated the daily estimates over periods of 1 week to reduce the computational burden and better assess the long-term statistics of the observations. As a final step, by using the GLORG module of GLOBK, weekly-averaged solutions and their full covariance matrices were combined to estimate a consistent set of positions and velocities in a fixed Eurasian reference frame. In this last step, to properly take into account for temporally correlated noise that generally affects the velocity uncertainty estimations, we adopted the first-order Gauss-Markov extrapolation (FOGMEX) algorithm proposed by Herring (2003). In particular, with FOGMEX method, after removing the best-fitting annual and semi-annual signals, a correlation time of the residuals for each coordinate component is estimated by computing the increase in the chi-squared-per-degree of freedom of successively longer time averages of the residuals. For a white noise error model, the chi-squared-per-degree of freedom would not depend on averaging time. With temporal correlations in the time series, chi-squared-per-degree of freedom increases as the residuals are averaged over successively longer time intervals. The estimated random walk for each component of each station was incorporated into the Kalman filter used to estimate the final site velocities. Estimated GPS velocities, referred to a fixed Eurasian reference frame (Cannavò and

Palano, 2015) and associated uncertainties at the 95% level of confidence are reported in Fig. 1.

References

Anderson, H.J., Jackson, J.A., 1987. The deep seismicity of the Tyrrhenian sea. Geophys. J. Int. 91, 613–637, http://dx.doi.org/10.1111/j.1365-246X.1987.tb01661.x.

Argnani, A., Armigliato, A., Pagnoni, G., Zaniboni, F., Tinti, S., Bonazzi, C., 2012. Active tectonics along the submarine slope of south-eastern Sicily and the source of the 11 January 1693 earthquake and tsunami. Nat. Hazards Earth Syst. Sci. 12, 1311–1319, http://dx.doi.org/10.5194/nhess-12-1311-2012.

Beutler, G., Moore, A.W., Mueller, I.I., 2008. The International Global Navigation Satellite Systems (GNSS) Service: developments and achievements. J. Geod. 83, 3307, http://dx.doi.org/10.1007/s00190-008-0268-z.

Baccheschi, P., Margheriti, L., Steckler, M.S., Boschi, E., 2011. Anisotropy patterns in the subducting lithosphere and in the mantle wedge: a case study. The southern Italy subduction system. J. Geophys. Res. 116, B08306, http://dx.doi.org/10.1029/2010JB007961.

Barreca, G., Scarfì, L., Cannavò, F., Koulakov, I., Monaco, C., 2016. New structural and seismological evidence and interpretation of a lithospheric-scale shear zone at the southern edge of the Ionian subduction system (central-eastern Sicily, Italy). Tectonics 35, 1489–1505, http://dx.doi.org/10.1002/2015TC004057.

Beccaluva, L., Bianchini, G., Coltorti, M., Siena, F., Verde, M., 2005. Cenozoic Tectono-Magmatic Evolution of the Central-Western Mediterranean: migration of an arc-interarc basin system and variations in the mode of subduction. In: Finetti, L.R. (Ed.), Crop-Deep Seismic Exploration of the Mediterranean Region. Elsevier, pp. 623–640.

Billi, A., Presti, D., Faccenna, C., Neri, G., Orecchio, B., 2007. Seismotectonics of the Nubia plate compressive margin in the south-Tyrrhenian region, Italy: clues for subduction inception. J. Geophys. Res. 112, B08302, http://dx.doi.org/10.1029/2006JB004837.

Billi, A., Presti, D., Orecchio, B., Faccenna, C., Neri, G., 2010. Incipient extension along the active convergent margin of Nubia in Sicily, Italy: Cefalù-Etna seismic zone. Tectonics 29, TC4026, http://dx.doi.org/10.1029/2009TC002559.

Calò, M., Parisi, L., Luzio, D., 2013. Lithospheric P- and S-wave velocity models of the Sicilian area using WAM tomography: procedure and assessments. Geophys. J. Int. 195, 625–649.

Cannavò, F., Palano, M., 2015. Defining Geodetic Reference Frame using Matlab: PlatEMotion 2.0. Pure Appl. Geophys., http://dx.doi.org/10.1007/s00024-015-1112-z.

Cannavò, F., Palano, M., 2016. Defining geodetic reference frame using matlab: platEMotion 2.0. Pure Appl. Geophys. 173 (3), 937–944, http://dx.doi.org/10.1007/s00024-015-1112-z.

Casero, P., Rour, F., Moretti, I., Endignoux, L., Muller, C., Sage, L., Vially, R., 1988. Neogene geodynamic evolution of the Southern Appennines. Mem. Soc. Geol. Ital. 41, 109–120.

Casero, P., 2004. Structural setting of petroleum exploration plays in Italy. In: Crescenti, et al. (Eds.), Geology of Italy. In: Soc. Geol. It. Spec. Vol, pp. 189–200.

Castello, B., Selvaggi, G., Chiarabba, C., Amato, A., 2006. CSI Catalogo Della Sismicità Italiana 1981–2002 Version 1.1. INGV-CNT, Roma (Available from) http://www.ingv.it/CSI/.

Cernobori, L., Hirn, A., McBride, J.H., Nicolich, R., Petronio, L., Romanelli, M., STREAMERS/PROFILES Working Groups, 1996. Crustal image of the Ionian basin and its Calabrian margins. Tectonophysics 264, 175–189, http://dx.doi.org/10.1016/S0040-1951(96)00125-4.

Chiarabba, C., Chiodini, G., 2013. Continental delamination and mantle dynamicsdrive topography, extension and fluid discharge in the Apennines. Geology 41, 715–718, http://dx.doi.org/10.1130/G33992.1.

Chiarabba, C., Jovane, L., Di Stefano, R., 2005. A new view of Italian seismicity using 20 years of instrumental recordings. Tectonophysics 395, 251–268, http://dx.doi.org/10.1016/j.tecto.2004.09.013.

Chiarabba, C., De Gori, P., Speranza, F., 2008. The southern Tyrrhenian subduction zone. Deep geometry, magmatism and Plio-Pleistocen evolution. Earth Planet. Sci. Lett. 268, 408–423, http://dx.doi.org/10.1016/j.epsl.2008.01.036.

Chiarabba, C., De Gori, P., Mele, F.M., 2015. Recent seismicity of Italy: active tectonics of the central Mediterranean region and seismicity rate changes after the Mw 6.3 L'Aquila earthquake. Tectonophysics 638, 82–93, http://dx.doi.org/10.1016/j.tecto.2014.10.016.

D'Argenio, B., Pescatore, T., Scandone, P., 1973. Schema geologico dell'Appennino Meridionale. Atti Convegno Moderne vedute sulla geologia dell'Appennino. Acc. Naz. Lincei 183, 49–72.

DeMets, C., Gordon, R.G., Argus, D.F., 2010. Geologically current plate motions. Geophys. J. Int. 181, 1–80, http://dx.doi.org/10.1111/j.1365-246X.2009.04491.x.

Dercourt, J., Zonenshain, L.P., Ricou, L.-E., Kazmin, V.G., Le Pichon, X., Knipper, A.L., Grandjacquet, C., Sbortshikov, I.M., Geyssant, J., Lepvrier, C., Pechersky, D.H., Boulin, J., Sibuet, J.-C., Savostin, L.A., Sorokthin, O., Westphal, M., Bazhenov, M.L., Lauer, J.P., Biju-Duval, B., 1986. Geological evolution of the Tethys belt from the Atlantic to the Pamirs since the Lias. Tectonophysics 123, 241–315, http://dx.doi.org/10.1016/0040-1951(86)90199-X.

Dewey, J.F., Helman, M.L., Knott, S.D., Turco, E., Hutton, D.H.W., 1989. Kinematics of the western Mediterranean. Geol. Soc. London, Sp. Pub. 45, 265–283, http://dx.doi.org/10.1144/GSL.SP.1989.045.01.15.

Doglioni, C., 1991. A proposal for the kinematic modelling of west-dipping subductions – possible applications to the Tyrrhenian-Apennines system. Terra Nova 3, 423–434.

Dow, J.M., Neilan, R.E., Rizos, C., 2009. The International GNSS Service in a changing landscape of Global Navigation Satellite Systems. J. Geod. 83 (3–4), 191–198, http://dx.doi.org/10.1007/s00190-008-0300-3.

Faccenna, C., Becker, T.W., 2010. Shaping mobile belts by small-scale convection. Nature 465, 602–605, http://dx.doi.org/10.1038/nature09064.

Faccenna, C., Becker, T.W., Lucente, F.P., Jolivet, L., Rossetti, F., 2001. History of subduction and back-arc extension in the central Mediterranean. Geophys. J. Int. 145, 809–820, http://dx.doi.org/10.1046/j.0956-540X.2001.01435.x.

Faccenna, C., Becker, T.W., Auer, L., Billi, A., Boschi, L., Brun, J.P., Capitanio, F.A., Funiciello, F., Horvàth, F., Jolivet, L., Piromallo, C., Leigh Royden, L., Rossetti, F., Serpelloni, E., 2014. Mantle dynamics in the Mediterranean. Rev. Geophys. 52, 283–332, http://dx.doi.org/10.1002/2013RG000444.

Finetti, I.R., Del Ben, A., 1996. Crustal tectono-Stratigraphic setting of the pelagian foreland from new CROP seismic data. In: Finetti, I.R. (Ed.), CROP PROJECT: Deep Seismic Exploration of the Central Mediterranean and Italy. Chapter 26., pp. 581–595.

Gallais, F., Graindorge, D., Gutscher, M.-A., Klaeschen, D., 2013. Propagation of a lithospheric tear fault (STEP) through the western boundary of the Calabrian accretionary wedge offshore eastern Sicily (southern Italy). Tectonophysics 602, 141–152, http://dx.doi.org/10.1016/j.tecto.2012.12.026.

Gattacceca, J., Speranza, F., 2002. Paleomagnetism of Jurassic to Miocene sediments from the Apenninic carbonate platform (southern Apennines, Italy): evidence for a 60° counterclockwise Miocene rotation. Earth Planet. Sci. Lett. 201, 19–34, http://dx.doi.org/10.1016/S0012-821X(02)00686-6.

Giacomuzzi, G., Chiarabba, C., De Gori, P., 2011. Linking the Alps and Apennines subduction systems: new constraints revealed by high-resolution teleseismic tomography. Earth Planet. Sci. Lett. 301 (3–4), 531–543, http://dx.doi.org/10.1016/j.epsl.2010.11.033.

Giacomuzzi, G., Civalleri, M., De Gori, P., Chiarabba, C., 2012. A 3D Vs model of the upper mantle beneath Italy: insight on the geodynamics of Central Mediterranean. Earth Planet. Sci. Lett. 335–336, 105–120, http://dx.doi.org/10.1016/j.epsl.2012.05.004.

Giunta, G., Luzio, D., Agosta, F., Calò, M., Di Trapani, F., Giorgianni, A., Oliveri, E., Orioli, S., Perniciaro, M., Vitale, M., Chiodi, M., Adelfio, G., 2009. An integrated approach to investigate the seismotectonics of northern Sicily and southern Tyrrhenian. Tectonophysics 476, 13–21, http://dx.doi.org/10.1016/j.tecto.2008.09.031.

Goes, S., Giardini, D., Jenny, S., Hollenstein, C., Kahle, H.-G., Geiger, A., 2004. A recent reorganization in the south-central Mediterranean. Earth Planet. Sci. Lett. 226, 335–345, http://dx.doi.org/10.1016/j.epsl.2004.07.038.

Govers, R., Wortel, M.J.R., 2005. Lithosphere tearing at STEP faults: reponse to edges of subduction zones. Earth Planet. Sci. Lett. 236, 505–523, http://dx.doi.org/10.1016/j.epsl.2005.03.022.

Gutscher, M.-A., Dominguez, S., Mercier de Lepinay, B., Pinheiro, L., Gallais, F., Babonneau, N., Cattaneo, A., Le Faou, Y., Barreca, G., Micallef, A., Rovere, M., 2016. Tectonic expression of an active slab tear from high-resolution seismic and bathymetric data offshore Sicily (Ionian Sea). Tectonics 34, 39–54, http://dx.doi.org/10.1002/2015TC003898.

Gutscher, M.-A., Kopp, H., Krastel, S., Bohrmann, G., Garlan, T., Zaragosi, S., Klaucke, I., Wintersteller, P., Loubrieu, B., LeFaou, Y., San Pedro, L., Dominguez, S., Rovere, M., Mercier de Lepinay, B., Ranero, C., Sallares, V., 2017. Active tectonics of the Calabrian subduction revealed by new multi-beam bathymetric data and high-resolution seismic profiles in the Ionian Sea (Central Mediterranean). Earth and Planet. Sci. Lett. 461, 61–72, http://dx.doi.org/10.1016/j.epsl.2016.12.020.

Herring, T.A., 2003. MATLAB Tools for viewing GPS velocities and time series. GPS Solutions 7 (3), 194–199, http://dx.doi.org/10.1007/s10291-003-0068-0.

Herring, T.A., King, R.W., McClusky, S.C., 2010. Introduction to GAMIT/GLOBK, Release 10.4. Massachusetts Institute of Technology, Cambridge, MA, pp. 1–48.

Jolivet, L., Augier, R., Robin, C., Suc, J.P., Rouchy, J.M., 2006. Lithospheric-scale geodynamic context of the Messinian salinity crisis. Sediment. Geol. 188–189, 9–33, http://dx.doi.org/10.1016/j.sedgeo.2006.02.004.

Lucente, F.P., Chiarabba, C., Cimini, G.B., Giardini, D., 1999. Tomographic constraints on the geodynamic evolution of the Italian region. J. Geophys. Res. 104, 20307–20327, http://dx.doi.org/10.1029/1999JB900147.

Lucente, F.P., Margheriti, L., Piromallo, C., Barruol, G., 2006. Seismic anisotropy reveals the long route of the slab through the western-central Mediterranean mantle. Earth Planet. Sci. Lett. 241, 517–529, http://dx.doi.org/10.1016/j.epsl.2005.10.041.

Lustrino, M., Melluso, L., Morra, V., 2000. The role of lower continental crust and lithospheric mantle in the genesis of Plio-Pleistocene volcanic rocks from Sardinia (Italy). Earth Planet. Sci. Lett. 180 (3–4), 259–270, http://dx.doi.org/10.1016/S0012-821X(00)00185-0.

Lustrino, M., Duggen, S., Rosenberg, C.L., 2011. The Central-Western Mediterranean: anomalous igneous activity in an anomalous collisional tectonic setting. Earth-Sci. Rev. 104, 1–40, http://dx.doi.org/10.1016/j.earscirev.2010.08.002.

Malinverno, A., Ryan, W.B.F., 1986. Extension in the Tyrrhenian Sea and shortening in the Apennines as result of arc migration driven by sinking of the lithosphere. Tectonics 5 (2), 227–245, http://dx.doi.org/10.1029/TC005i002p00227.

Mattei, M., Cifelli, F., D'Agostino, N., 2007. The evolution of the Calabrian Arc: evidence from paleomagnetic and GPS observations. Earth Planet. Sci. Lett. 263, 259–274, http://dx.doi.org/10.1016/j.epsl.2007.08.034.

Minelli, L., Faccenna, C., 2010. Evolution of the calabrian accretionary wedge (central mediterranean). Tectonics, TC4004, http://dx.doi.org/10.1029/2009TC002562.
Musumeci, C., Scarfì, L., Palano, M., Patanè, D., 2014. Foreland segmentation along an active convergent margin: new constraints in southeastern Sicily (Italy) from seismic and geodetic observations. Tectonophysics 630, 137–149, http://dx.doi.org/10.1016/j.tecto.2014.05.017.
Neri, G., Orecchio, B., Totaro, C., Falcone, G., Presti, D., 2009. Subduction beneath southern Italy is close to ending: results from seismic tomography. Seism. Res. Lett. 80, 63–70, http://dx.doi.org/10.1785/gssrl.80.1.63.
Neri, G., Marotta, A.M., Orecchio, B., Presti, D., Totaro, C., Barzaghi, R., Borghi, A., 2012. How lithospheric subduction changes along the Calabrian Arc in southern Italy: geophysical evidences. Int. J. Earth Sci. 101, 1949–1969 (1007/s00531-012-0762-7).
Nicolosi, I., Speranza, F., Chiappini, M., 2006. Ultrafast oceanic spreading of the Marsili Basin, southern Tyrrhenian Sea: evidence from magnetic anomaly analysis. Geology 34, 717–720, http://dx.doi.org/10.1130/G22555.1.
Nocquet, J.M., Calais, E., 2003. Crustal velocity field of western Europe from permanent GPS array solutions, 1996–2001. Geophys. J. Int. 154, 72–88, http://dx.doi.org/10.1046/j.1365-246X.2003.01935.x.
Palano, M., Ferranti, L., Monaco, C., Mattia, M., Aloisi, M., Bruno, V., Cannavò, F., Siligato, G., 2012. GPS velocity and strain fields in Sicily and southern Calabria, Italy: updated geodetic constraints on tectonic block interaction in the central Mediterranean. J. Geophys. Res. 117, B07401, http://dx.doi.org/10.1029/2012JB009254.
Palano, M., Schiavone, D., Loddo, M., Neri, M., Presti, D., Quarto, R., Totaro, C., Neri, G., 2015. Active upper crust deformation pattern along the southern edge of the Tyrrhenian subduction zone (NE Sicily): Insights from a multidisciplinary approach. Tectonophysics 657, 205–218, http://dx.doi.org/10.1016/j.tecto.2015.07.005.
Palano, M., Piromallo, C., Chiarabba, C., 2017. Surface imprint of toroidal flow at retreating slab edges: the first geodetic evidence in the Calabrian subduction system. Geophys. Res. Lett. 44, http://dx.doi.org/10.1002/2016gl071452.
Palano, M., 2015. On the present-day crustal stress, strain-rate fields and mantle anisotropy pattern of Italy. Geophys. J. Int. 200 (2), 969–985, http://dx.doi.org/10.1093/gji/ggu451.
Patacca, E., Sartori, R., Scandone, P., 1990. Tyrrhenian basin and Apenninic arcs. Kinematic relations since late Tortonian times. Mem. Soc. Geol. Ital. 45, 425–451.
Piromallo, C., Morelli, A., 2003. P wave tomography of the mantle under the Alpine-Mediterranean area. J. Geophys. Res. 108, 2065, http://dx.doi.org/10.1029/2002JB001757.
Polonia, A., Torelli, L., Mussoni, P., Gasperini, L., Artoni, A., Klaeschen, D., 2011. The Calabrian Arc subduction complex in the Ionian Sea: regional architecture, active deformation, and seismic hazard. Tectonics 30, TC5018, http://dx.doi.org/10.1029/2010tc002821.
Polonia, A., Torelli, L., Artoni, A., Carlini, M., Faccenna, C., Ferranti, L., Gasperini, L., Klaeschen, D., Monaco, C., Neri, G., Nijholt, N., Orecchio, B., Wortel, R., Govers, R., 2016. The Ionian and Alfeo-Etna fault zones: new segments of an evolving plate boundary in the central Mediterranean Sea? Tectonophysics 675, 69–90, http://dx.doi.org/10.1016/j.tecto.2016.03.016.
Pondrelli, S., Piromallo, C., Serpelloni, E., 2004. Convergence vs. retreat in Southern Tyrrhenian Sea: insights from kinematics. Geophys. Res. Lett. 31 (6), L06611, http://dx.doi.org/10.1029/2003GL019223.
Rosenbaum, G., Lister, G.S., 2004. Neogene and Quaternary rollback evolution of the Tyrrhenian Sea, the Apennines and the Sicilian Maghrebides. Tectonics 23, TC1013, http://dx.doi.org/10.1029/2003tc001518.
Rosenbaum, G., Lister, G., Duboz, C., 2002. Reconstruction of the tectonic evolution of the western Mediterranean since the Oligocene. J. Virtual Explor. 8, 107–130, http://dx.doi.org/10.3809/jvirtex.2002.00053.
Rosenbaum, G., Gasparon, M., Lucente, F.P., Peccerillo, A., Miller, M.S., 2008. Kinematics of slab tear faults during subduction segmentation implications for Italian magmatism. Tectonics 27, TC2008, http://dx.doi.org/10.1029/2007TC002143.
Rovida, A., Camassi, R., Gasperini, P., Stucchi, M., 2011. CPTI11, the 2011 Version of the Parametric Catalogue of Italian Earthquakes., http://dx.doi.org/10.6092/INGV.IT-CPTI11 (Milano, Bologna) http://emidius.mi.ingv.it/CPTI.
Savelli, C., 2002. Time-space distribution of magmatic activity in the western Mediterranean and peripheral orogens during the past 30 Ma (a stimulus to geodynamic considerations). J. Geodyn. 34, 99–126, http://dx.doi.org/10.1016/S0264-3707(02)00026-1.
Selvaggi, G., Chiarabba, C., 1995. Seismicity and P-velocity image of the southern Tyrrhenian subduction zone. Geophys. J. Int. 121, 818–826, http://dx.doi.org/10.1111/j.1365-246X.1995.tb06441.x.
Speranza, F., Villa, I.M., Sagnotti, L., Florindo, F., Cosentino, D., Cipollari, P., Mattei, M., 2002. Age of the Corsica-Sardinia rotation and Liguro-Procençal Basin spreading: new paleomagnetic and Ar/Ar evidence. Tectonophysics 347, 231–251, http://dx.doi.org/10.1016/S0040-1951(02)00031-8.
Stampfli, G.M., 2000. Tethyan oceans. In: Bozkurt, E., Winchester, J.A., Piper, J.D.A. (Eds.), Tectonics and Magmatism in Turkey and Surrounding Area, 173. Geol. Soc. London, Sp. Pub., pp. 163–185.
Wortel, M.J.R., Spakman, W., 2000. Subduction and slab detachment in the Mediterranean-Carpathian Region. Science 290, 1917–1920, http://dx.doi.org/10.1126/science.290.5498.1910.
Wortel, M.J.R., Govers, R., Spakman, W., 2009. Continental collision and the STEP-wise evolution of convergent plate boundaries: from structure to dynamics. In: Lallemand, S., Funicello, F. (Eds.), Subduction Zone Geodynamics. Springer-Verlag, Berlin Heidelberg, pp. 47–59.